agriculture

MDPI

Article

Responses of Soybean Water Supply and Requirement to Future Climate Conditions in Heilongjiang Province

Na Li [1], Tangzhe Nie [1,2,*], Yi Tang [1], Dehao Lu [1], Tianyi Wang [3], Zhongxue Zhang [2,3], Peng Chen [4], Tiecheng Li [2,3], Linghui Meng [5], Yang Jiao [1] and Kaiwen Cheng [1]

1 School of Water Conservancy and Electric Power, Heilongjiang University, Harbin 150080, China; 2201954@s.hlju.edu.cn (N.L.); 2201943@s.hlju.edu.cn (Y.T.); 2212006@s.hlju.edu.cn (D.L.); 2201957@s.hlju.edu.cn (Y.J.); 20195777@s.hlju.edu.cn (K.C.)
2 Key Laboratory of Efficient Use of Agricultural Water Resources, Ministry of Agriculture and Rural Affairs, Northeast Agricultural University, Harbin 150030, China; zhangzhongxue@neau.edu.cn (Z.Z.); b210101005@neau.edu.cn (T.L.)
3 School of Water Conservancy and Civil Engineering, Northeast Agricultural University, Harbin 150030, China; 2191532@s.hlju.edu.cn
4 College of Agricultural Science and Engineering, Hohai University, Nanjing 210098, China; 190210070001@hhu.edu.cn
5 School of Architecture and Engineering, Liaocheng University, Liaocheng 252000, China; m15762134644@163.com
* Correspondence: 2019036@hlju.edu.cn; Tel.: +86-189-4508-3525

Abstract: Understanding future changes in water supply and requirement under climate change is of great significance for long-term water resource management and agricultural planning. In this study, daily minimum temperature (T_{min}), maximum temperature (T_{max}), solar radiation (Rad), and precipitation for 26 meteorological stations under RCP4.5 and RCP8.5 of MIRCO5 for the future period 2021–2080 were downscaled by the LARS-WG model, daily average relative humidity (RH) was estimated using the method recommended by FAO-56, and reference crop evapotranspiration (ET_0), crop water requirement (ET_c), irrigation water requirement (I_r), effective precipitation (P_e), and coupling degree of ET_c and P_e (CD) for soybean during the growth period were calculated by the CROPWAT model in Heilongjiang Province, China. The spatial and temporal distribution of these variables and meteorological factors were analyzed, and the response of soybean water supply and requirement to climate change was explored. The result showed that the average T_{min}, T_{max}, and Rad under RCP4.5 and RCP8.5 increased by 0.2656 and 0.5368 °C, 0.3509 and 0.5897 °C, and 0.0830 and 0.0465 MJ/m^2, respectively, while the average RH decreased by 0.0920% and 0.0870% per decade from 2021 to 2080. The annual average ET_0, ET_c, P_e, and I_r under RCP4.5 for 2021–2080 were 542.89, 414.35, 354.10, and 102.44 mm, respectively, and they increased by 1.92%, 1.64%, 2.33%, and −2.12% under the RCP8.5, respectively. The ranges of CD under RCP4.5 and RCP8.5 were 0.66–0.95 and 0.66–0.96, respectively, with an average value of 0.84 for 2021–2080. Spatially, the CD showed a general trend of increasing first and then decreasing from west to east. In addition, ET_0, ET_c, and P_e increased by 9.55, 7.16, and 8.77 mm per decade, respectively, under RCP8.5, while I_r decreased by 0.65 mm per decade. Under RCP4.5 and RCP8.5, ET_c, P_e, and I_r showed an overall increasing trend from 2021 to 2080. This study provides a basis for water resources management policy in Heilongjiang Province, China.

Keywords: climate change; soybean; CROPWAT; reference crop evapotranspiration (ET_0); crop water requirement (ET_c); irrigation water requirement (I_r)

check for updates

Citation: Li, N.; Nie, T.; Tang, Y.; Lu, D.; Wang, T.; Zhang, Z.; Chen, P.; Li, T.; Meng, L.; Jiao, Y.; et al. Responses of Soybean Water Supply and Requirement to Future Climate Conditions in Heilongjiang Province. *Agriculture* **2022**, *12*, 1035. https://doi.org/10.3390/agriculture12071035

Academic Editors: Dengpan Xiao and Wenjiao Shi

Received: 23 May 2022
Accepted: 14 July 2022
Published: 15 July 2022

Publisher's Note: MDPI stays neutral with regard to jurisdictional claims in published maps and institutional affiliations.

1. Introduction

Global climate change, marked mainly by climate warming, has taken place [1]. Undoubtedly, this change has had and will continue to have an important impact on agricultural water resources on which crop growth depends [2]. In addition, climate

factors, such as relative humidity (*RH*), solar radiation (*Rad*), and CO_2 concentration, have a significant effect on crop water requirements (ET_c) [3]. Moreover, the uncertainty of temporal and spatial distribution of precipitation (P) and ET_c affects crop irrigation water requirement (I_r) [4]. Therefore, analyzing the impact of future climatic changes on crop water supply and requirement becomes necessary [5].

Future climate change is expected to affect water supply and requirement in a number of ways [6]. Climate change mainly affects the transpiration of plants, evaporation of water from the soil and field surface between plants, and P in the agricultural water cycle system [7]. *Rad* is the largest source of energy required for soil water vaporization during evapotranspiration, which converts a large amount of liquid water into water vapor. *Rad* absorbed by the atmosphere and heat emitted from the surface increase the atmospheric temperature [8]. The sensible heat around the atmosphere transmits energy to the crop to control the evapotranspiration rate, and the increase in soil surface temperature promotes evaporation [5]. The water vapor pressure difference between the evapotranspiration surface and the atmosphere is the decisive factor for water vapor movement [9]. The increase in *RH* leads to the saturation of air humidity, forming a protective layer on the field surface, thus reducing the evapotranspiration requirement [10]. However, the increase in CO_2 concentration will also promote the accumulation of crop dry matter, promote plant growth, and increase transpiration [11]. P increases soil water content, replenishes the total effective soil water, improves the plant root water absorption rate, and helps to reduce I_r while meeting the needs of crop evapotranspiration [12]. Some researchers found that the *RH* in Zimbabwe areas would decrease in the future, while the average temperature, *Rad* and wind speed would increase, resulting in an increase in ET_0 and ET_c; however, the decrease in P would eventually lead to the increase of I_r [13]. In contrast, studies in North China Plain (NCP) found that ET_c and I_r decreased with increasing temperature, *Rad* and P, shorten of growth period [14]. In many studies from different regions, the relationships between ET_c, P_e, and I_r varies under climate change. Therefore, more in-depth studies are needed to assess the impact of future climate change on crop water supply and requirement.

ET_c constitutes a major component of regional and global hydrological cycles and, therefore, has important implications in the use of agricultural irrigation water, as well as in analyzing the crop water supply and requirement relationship in agricultural ecosystems [15]. There are many methods for calculating ET_c, such as the empirical estimation method, the Penman–Monteith (P–M) double-crop coefficient method, and the P–M single-crop coefficient method [16]. The empirical formula for estimating ET_c is simple and convenient; however, it is only suitable for local instead of large-scale areas [17]. When using P–M double-crop coefficient method to estimate ET_c, the crop coefficient is divided into basic crop coefficient (K_{cb}) and soil evaporation coefficient (K_e), although the estimation accuracy of ET_c is improved [18]; however, the estimation of K_e is complex and uncertain, which needs the support of a large amount of experimental data [19,20]. The parameters required by the P–M single-crop coefficient method are easy to obtain, which can be directly substituted into the formula for calculation. The calculated ET_c has less difference with the measured ET_c. Generally, the P–M single-crop coefficient method has strong universality in different regions and is considered to be a more efficient, convenient, and accurate method [21,22]. Therefore, most scholars use the P–M single-crop coefficient method recommended by the Food and Agriculture Organization of the United Nations (FAO) to calculate ET_c [23]. Nie et al. estimated rice ET_c in Heilongjiang province using the CROPWAT model based on the P–M single-crop coefficient method [24]; the calculated ET_c was only 21–30 mm different from the measured ET_c in the field experiment. In order to test the practicability and rationality of the P–M single-crop coefficient method for calculating ET_c, Jin et al. calculated wheat ET_c in the Huaihongxinhe Irrigation District using the P–M single-crop coefficient method and found that the average difference in ET_c for the years was only 6 mm [25].

Quantitative estimation of temporal and spatial variability of ET_c, P_e, and I_r under climate change is helpful to maximize the use of rainwater resources and optimize regional water resource allocation [11,14]. P is the main influencing factor of soil moisture content, which provides water for crop evapotranspiration [26]. I_r depends on soil moisture content [27]. Therefore, there is a complex relationship between P_e and I_r, which cannot be fully explained by simple linear equations [28]. In addition, the relationship among ET_c, P_e, and I_r is also affected by P distribution pattern, crop species, and planting area [11]. In the Jayakwadi command area, India, the ET_c of major crops and P_e increased during the growth period, resulting in less I_r under climate change [29]. In the Najafabad plain in Iran, ET_c increased and P_e decreased during the growth period of major crops; therefore, more water needed to be irrigated [30].

As one of the largest developing countries in the world, China constitutes 22% of the world's population and encompasses 9% of the world's arable land [31]. Heilongjiang Province has the largest arable land area in China and is also an important commercial grain base in China [32]. The soybean sowing area and yield in Heilongjiang Province rank first in China, with a sowing area of 4.279×10^6 ha and yield of 7.808×10^6 tons as of 2019 [33]. Soybean sowing area increased by an average of 5×10^5 ha per year in the last 5 years. The climate distribution in Heilongjiang province leads to great differences in temporal and spatial distribution of crop water supply and requirement, and agricultural drought occurs frequently in spring and summer [34]. With the increase in soybean planting area and soybean export share, the study on soybean water supply and requirement under future climatic conditions is of great guidance to ensure soybean production and food security in Heilongjiang Province [35].

The purpose of this study was (1) to clarify the spatial and temporal distribution characteristics of ET_0, ET_c, P_e, I_r, and CD during the soybean growth period for 2021–2080 under RCP4.5 and RCP8.5 in Heilongjiang Province, and (2) to reveal the response of soybean water supply and requirement to climate change for 2021–2080 under RCP4.5 and RCP8.5. This study will provide reasonable planning for water allocation and guide the sustainable development of agricultural irrigation water use in Heilongjiang Province.

2. Materials and Methods

2.1. Study Region and Datasets

The study area is located in Heilongjiang Province, Northeast China, where 26 meteorological stations are located relatively evenly throughout the study area for observations (Figure 1). The area belongs to the cold temperate and temperate continental monsoon climate, with an average annual temperature of 4.52 °C, an average annual solar radiation of 13.72 MJ/m^2, and an average annual P of 511 mm. According to the "Heilongjiang Province Crop Variety Cumulative Temperature Zone Plan" [36] and "Heilongjiang Province 2015 Regional Layout Plan for High-Quality and High-Yielding Major Food Crops" [37] issued by the Heilongjiang Provincial Agriculture Committee, the sixth cumulative temperature zone is not suitable for soybean cultivation; therefore, the sixth cumulative temperature zone is not included in this study.

We used the general circulation model (GCM) of MIRCO5 with a resolution of $1.39^\circ \times 1.41^\circ$ and selected two representative concentration pathways (RCP4.5 for the low-radiation scenario and RCP8.5 for the high-radiation scenario) according to the socioeconomic conditions of the radiative forcing currently faced by humans. The minimum temperature (T_{min}), maximum temperature (T_{max}), Rad, and P data from 26 stations of the China Meteorological Administration (CMA) from 1960–2015 were imported into the LARSWG stochastic weather generator model to generate future climate datasets. The dataset includes daily T_{min}, T_{max}, Rad, and P for 26 meteorological stations under RCP4.5 and RCP8.5 for the future period (2021–2080). The period 2021–2080 was divided into three time periods: the 2030s (2021–2040), 2050s (2041–2060), and 2070s (2061–2080). Under RCP4.5 and RCP8.5, average RH was estimated using the method recommended by FAO-56.

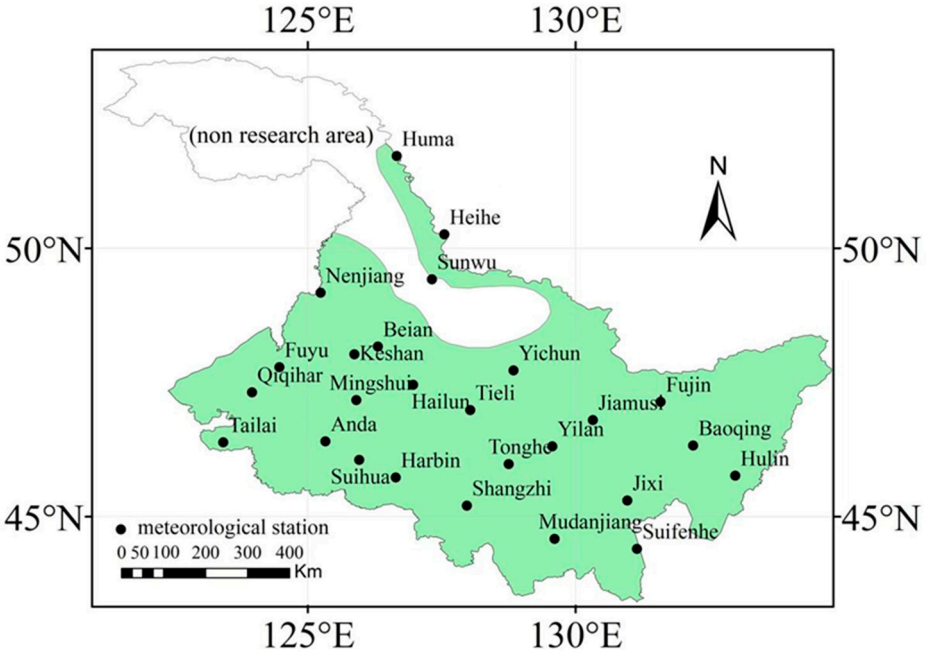

Figure 1. Study area and distribution of 26 meteorological stations in Heilongjiang Province.

2.2. Division of Soybean Growth Period

The FAO divides the crop growth period into four stages: initial stage (L_{ini}), crop development stage (L_{dev}), mid-season stage (L_{mid}), and late stage (L_{late}); the crop coefficients in each growth stage are K_{cini}, K_{cmid} and K_{cend}. In this study, the whole growth period of soybean was divided into sowing to three-leaf stage (L_{ini}), three-leaf stage to flowering stage (L_{dev}), flowering stage to podding stage (L_{mid}), and podding stage to maturity stage (L_{late}). The crop coefficients (K_c) were based on the irrigation series "Crop Guide to Crop Water Requirements" published by FAO-56 and corrected using the method recommended by FAO-56 [38,39]. It was assumed that the soybean variety would not change in the future period. According to the observation data of soybean growth period from 1994 to 2005 at 19 agrometeorological observation stations in Heilongjiang Province, the soybean sowing date and the length of each growth stage were determined. The data of the adjacent agrometeorological observation stations in the same temperature accumulation area were selected as the calculation basis, as shown in Table 1.

Table 1. Average soybean growth period data in 1994–2005.

Agrometeorological Station	L_{ini} (Days)	L_{dev} (Days)	L_{mid} (Days)	L_{Late} (Days)	Total Growth Day (Days)	Meteorological Station
Qinggang	24	31	59	16	130	Anda, Suihua
Hulin	27	30	60	17	134	Hulin
Boli	35	24	16	16	125	Jixi, Mudanjiang, Suifenhe
Bayan	29	24	62	23	138	Tonghe, Shangzhi
Heihe	32	25	59	17	133	Heihe, Sunwu
Harbin	34	32	67	17	150	Haerbin
Nenjiang	29	27	60	17	133	Nenjiang
Longjiang	20	27	63	22	132	Qiqihar, Tailai
Huma	33	18	57	17	125	Huma

Table 1. *Cont.*

Agrometeorological Station	L_{ini} (Days)	L_{dev} (Days)	L_{mid} (Days)	L_{Late} (Days)	Total Growth Day (Days)	Meteorological Station
Qingan	28	21	63	28	140	Tieli
Tangyuan	27	28	65	16	136	Yinlan
Beian	28	26	65	15	134	Keshan, Beian
Baiquan	27	27	55	23	132	Mingshui
Jiayin	30	24	57	16	127	Yichun
Hailun	28	29	63	19	139	Hailun
Jiamusi	28	32	62	17	139	Jiamusi
Fuyu	32	32	57	14	135	Fuyu
Baoqing	22	28	60	19	129	Baoqing
Fujin	29	25	60	21	135	Fujin

2.3. Soil Parameters

Parameters such as soil type, total available soil moisture, maximum rain infiltration rate, and maximum rooting depth were obtained from the Harmonized World Soil Database (HSWD). To improve the accuracy of the model simulation results, the initial soil moisture depletion and initial available soil moisture were adjusted according to the "10 day dataset of crop growth and development and farmland soil moisture in China" from the China Meteorological Data Network (http://data.cma.cn, accessed on 22 May 2022). The obtained soil data were input into the CROPWAT model, and the initial soil water content for each year thereafter was taken as the last day of the previous year.

2.4. Effective Precipitation (P_e)

For upland crops, P_e refers to the total precipitation that can be stored in the crop root layer to meet the crop's water needs, excluding surface runoff and leakage below the crop root layer. In this study, we used the method recommended by the United States Department of Agriculture (USDA) to calculate P_e. The formula was as follows:

$$P_e = \begin{cases} P(125 - 0.6P)/125 & (P \leq 83.3 \text{ mm}) \\ 125/3 + 0.1P & (P > 83.3 \text{ mm})' \end{cases} \quad (1)$$

where P_e is the effective precipitation (mm), and P is precipitation (mm).

2.5. Crop Water Requirement (ET_c)

Soybean ET_c was calculated using the CROPWAT model as a function of the loading altitude, latitude, longitude, T_{min}, T_{max}, Rad, and RH data from each station into the "climate/ET_0" module to calculate ET_0. The sowing date, harvest date, K_c, and length of each growing period were loaded into the "crop" module to calculate ET_c. Soybean ET_c was calculated using the single-crop coefficient method recommended by FAO-56. ET_c was calculated from ET_0 and K_c using the equation under standard conditions, where ET_0 was considered as the key variable for the estimation of ET_c. Standard conditions mean that there were no limitations to crop growth, including a sufficient supply of water and crops free from diseases and pest infections.

$$ET_c = K_c \times ET_0, \quad (2)$$

where ET_0 is the reference crop evapotranspiration (mm), K_c is the crop coefficient (dimensionless), and ET_c is the crop water requirement (mm).

ET_0 was calculated using the P–M formula recommended by FAO; thus,

$$ET_0 = \frac{0.408\Delta \times (R_n - G) + \frac{900\gamma \times u_2 \times (e_s - e_a)}{(T+273)}}{\Delta + \gamma \times (1 + 0.34u_2)}, \quad (3)$$

where ET_0 is the reference crop evapotranspiration (mm·day^{-1}), Δ is the slope of the vapor pressure curve (kPa·°C^{-1}), R_n is the net radiation at the crop surface (MJ·(m^2·day^{-1})), G is the soil heat flux density (MJ·(m^2·day^{-1})), γ is the psychrometric constant (kPa·°C^{-1}), T is the mean daily air temperature at 2 m height (°C), u_2 is the wind speed at 2 m height (m·s^{-1}), e_s is the saturation vapor pressure, e_a is the actual vapor pressure (kPa), $e_s - e_a$ is the saturation vapor pressure deficit (kPa), and 900 is a conversion factor.

2.6. Irrigation Water Requirement (I_r)

The daily soil water balance equation was used to calculate I_r. Irrigation quota should be less than or equal to the root-zone water consumption to avoid deep leakage loss. The calculation formula is as follows:

$$I_{r,i} = D_{r,i-1} + ET_c - D_{r,i} - P_{e_i}, \tag{4}$$

where $I_{r,i}$ is the irrigation water requirement on day i, $D_{r,i-1}$ is the water consumption of the root zone on day $i-1$, ET_c is crop water requirement, $D_{r,i}$ is the water consumption of the root zone on day i, and P_{ei} is the P_e on day i.

2.7. Climate Tendency Rate

The climate tendency rate is the changing rate of each variable every 10 years. A positive climate tendency rate indicates an increasing trend of the corresponding variable, while a negative value indicates a decreasing trend. By using the least-square method, the changing trend of variable can be expressed by a linear equation formulas follows:

$$Y_t = at + b, \tag{5}$$

where Y_t is represents the fitted values of each variable, t is the corresponding year, and a and b are regression coefficients.

2.8. Coupling Degree of ET_c and P_e (CD)

During the soybean growth period, the degree to which P_e meets ET_c is called the coupling degree between ET_c and P_e. The calculation equation is as follows:

$$\lambda_i = \begin{cases} 1 & (P_e \geq ET_c) \\ P_e/ET_c & (P_e < ET_c) \end{cases}. \tag{6}$$

2.9. Mann–Kendall Trend Test

The Mann–Kendall trend test is a nonparametric statistical method used to reveal how a variable changes with time, introduced by the World Meteorological Organization. Positive and negative values of the statistical variable Z indicate the data changing trend; if the absolute value of Z is greater than 1.64, 2.32, and 2.56, it means that the data have passed the significance test of 95%, 99%, and 99.9% for reliability [40]. This study used this method to test the changing trend of ET_0, ET_c, I_r, P_e, and CD during the soybean growth period.

2.10. Data Processing

The reduced-dimension downscaled dataset was processed by Codeblocks20.03 [41] open-source software, which made the data schema acceptable to the CROPWAT model. The CROPWAT8.0 [42] model was used to calculate ET_c, P_e, and I_r under future climate conditions at 26 meteorological stations in Heilongjiang Province. Matlab R2019a [43] was used to perform Mann–Kendall trend tests of ET_0, ET_c, P_e, I_r, and their climate tendency rates under future climatic conditions, and the inverse distance weighting (IDW) method in the spatial analysis toolbox of Arcmap 10.2 was used to spatially interpolate and mapping at a resolution of 0.04° × 0.04°. We used SPSS25.0 [44] to process the correlation analysis

of T_{min}, T_{max}, RH, Rad, ET_0, ET_c, P_e, and I_r, as well as the analysis of variance (ANOVA) of T_{min}, T_{max}, P_e, RH, Rad, ET_0, ET_c, I_r, and CD.

3. Results

3.1. Spatial and Temporal Variation of Future Meteorological Factor

ET_0 during the soybean growth period was driven by interacting effects of different climate factors. Therefore, a detailed analysis of changes for each meteorological factor was conducted (Figures 2 and 3). Average T_{max} under RCP4.5 and RCP8.5 showed a significant increasing trend, Rad showed an increasing and then decreasing trend, and average RH showed a decreasing and then increasing trend (Figure 2). Under RCP4.5 and RCP8.5, the average T_{max} started from 25.19 and 25.36 °C in the 2030s, respectively, and increased significantly to 26.76 and 28.02 °C in the 2070s. Similarly, the average Rad increased significantly from 21.04 and 21.15 MJ/m^2 in the 2030s to 21.56 and 21.53 MJ/m^2 in the 2050s, respectively, and then both decreased to 21.42 MJ/m^2 in the 2070s. The average RH decreased significantly from 75.07% and 74.92% in the 2030s to 74.36% and 74.42% in the 2050s, before continuing to increase to 74.50% and 74.65% in the 2070s, respectively. Under RCP4.5 and RCP8.5, the highest values of the T_{min} were distributed in the east, and the highest values of the T_{max} were distributed in the south. In addition, the highest RH was found in the central part, and the highest Rad was found in the western and eastern parts.

Under RCP4.5, the average climate tendency rates of T_{min}, T_{max}, RH, and Rad for 2021–2080 were 0.2656 °C/(10 years), 0.3509 °C/(10 years), −0.0920%/(10 years), and 0.0830 MJ/m^2/(10 years), respectively (Figure 3). Under RCP8.5, the average climate tendency rates of T_{min}, T_{max}, RH, and Rad in 2021–2080 were 0.5368 °C/(10 years), 0.5897 °C/(10 years), −0.0870%/(10 years), and 0.0465 MJ/m^2/(10 years), respectively. Under RCP4.5 from 2021–2050, the RH declined most quickly, at a rate of 0.3002%/(10 years), while Rad increased most quickly, at a rate of 0.2193 MJ/m^2/(10 years).

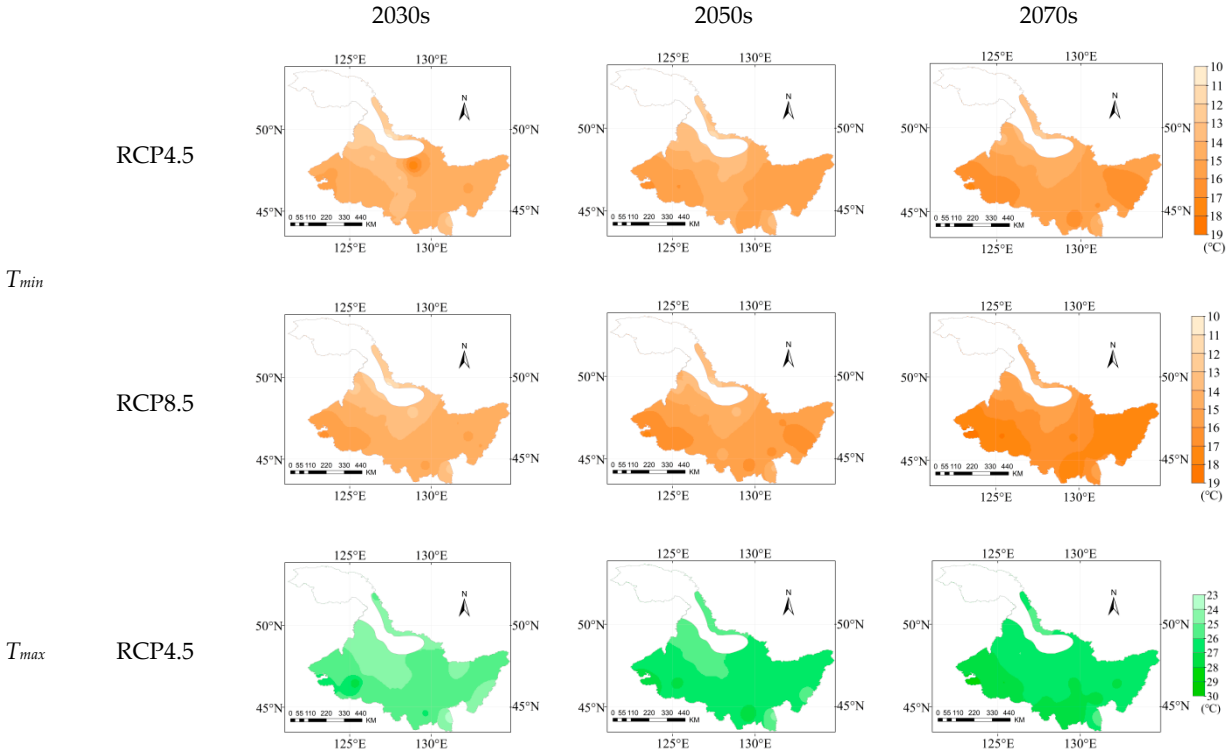

Figure 2. *Cont.*

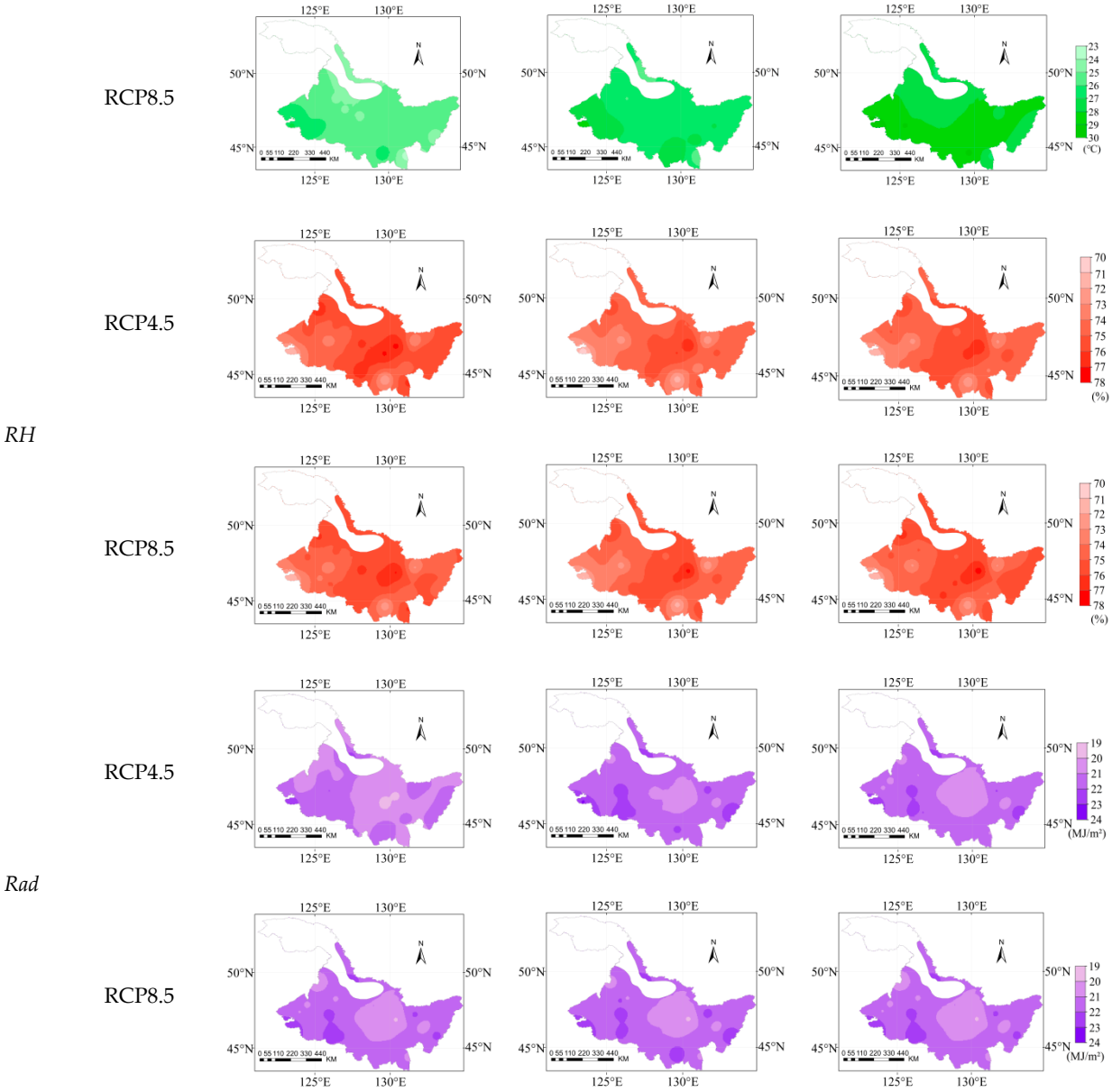

Figure 2. Spatial distribution of average minimum temperature (T_{min}), maximum temperature (T_{max}), relative humidity (*RH*), and solar radiation (*Rad*) during soybean growth period under RCP4.5 and RCP8.5 in the study area in the 2030s, 2050s, and 2070s.

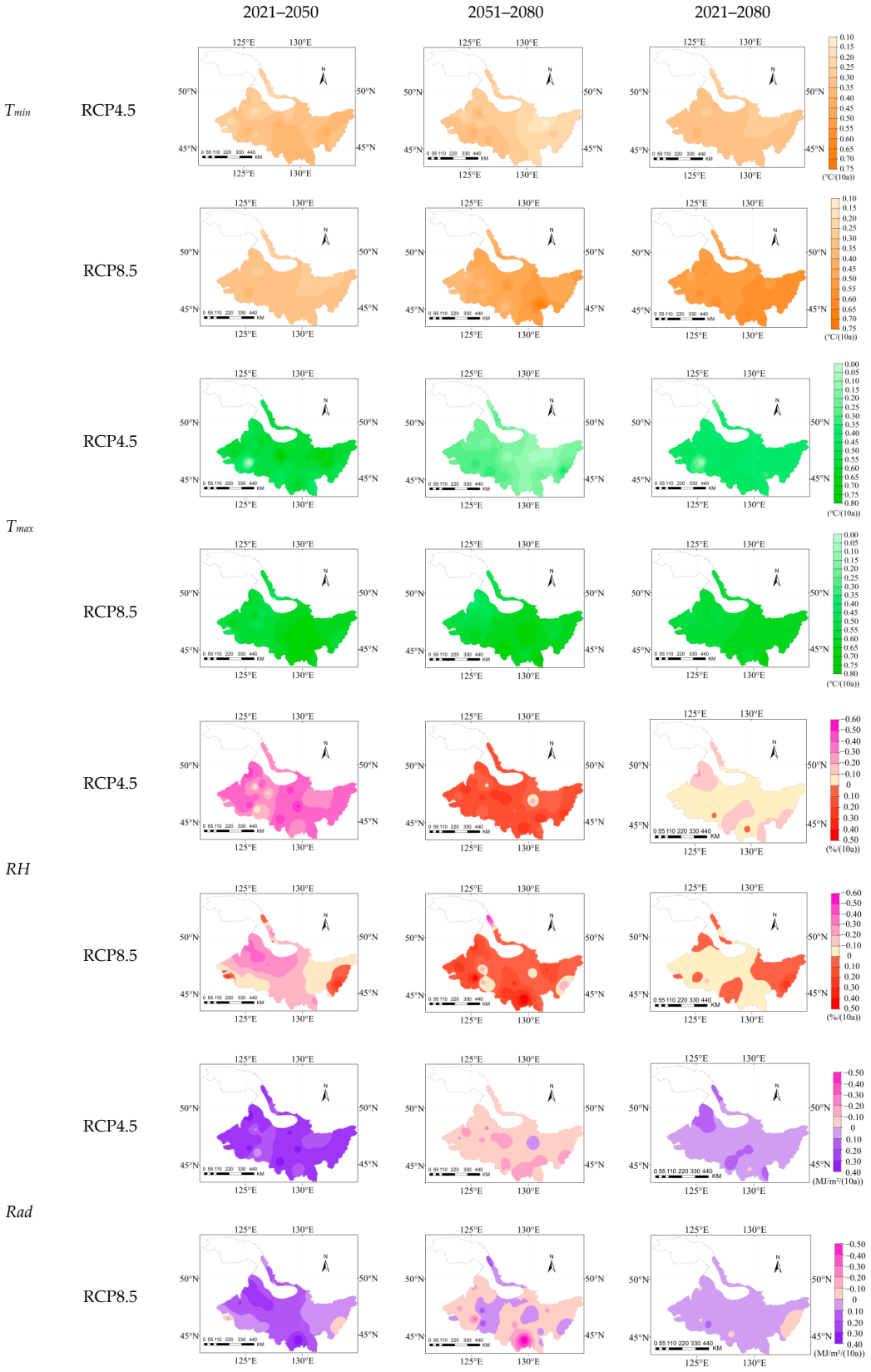

Figure 3. Climate tendency rates of average minimum temperature (T_{min}), maximum temperature (T_{max}), relative humidity (*RH*), and solar radiation (*Rad*) during soybean growth period under RCP4.5 and RCP8.5 in the study area in 2021–2050, 2051–2080, and 2021–2080.

3.2. Spatial and Temporal Variation of ET_0

The ET_0 values during the soybean growth period from 2021–2080 under RCP4.5 and RCP8.5 were shown in Figure 4. Under RCP4.5, ET_0 from 2021–2080 was between 409.34 and 621.47 mm, with an average of 542.89 mm. Under RCP8.5, ET_0 was between 492.48 and 642.24 mm, with an average of 553.35 mm. Under RCP4.5 and RCP8.5, ET_0 increased first and then decreased from west to east in the study area.

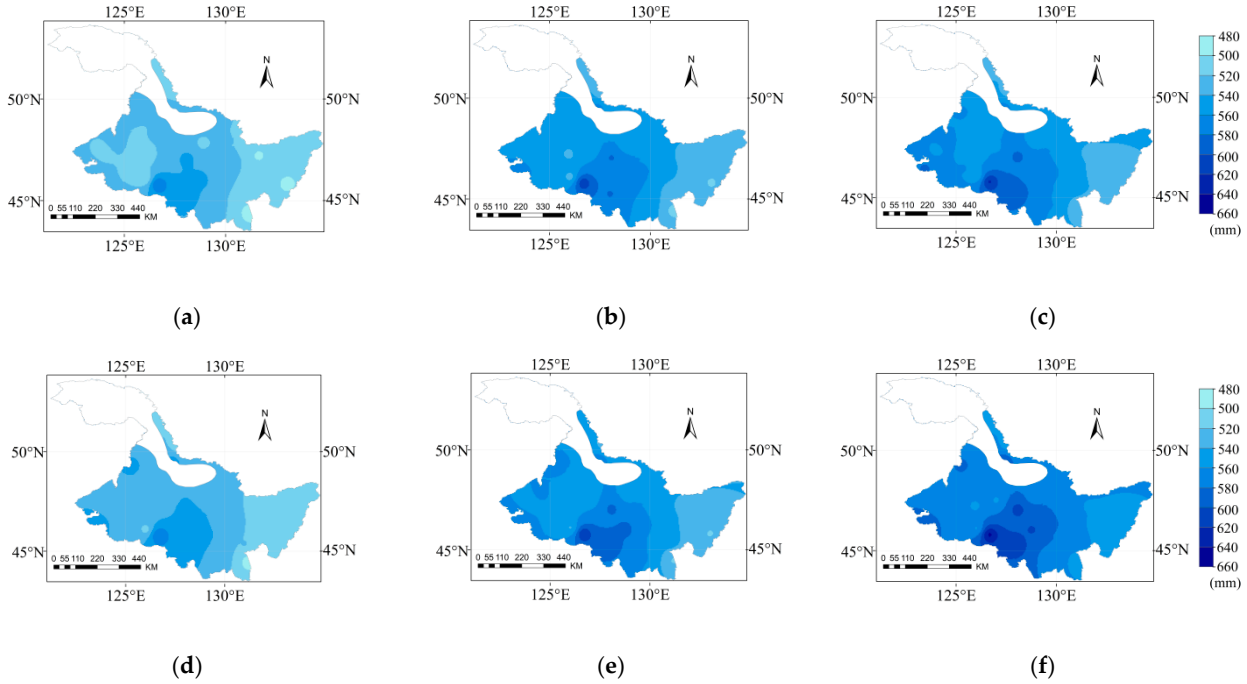

Figure 4. Spatial distribution of reference crop evapotranspiration (ET_0) during the (**a**) 2030s, (**b**) 2050s, and (**c**) 2070s under RCP4.5, and during the (**d**) 2030s, (**e**) 2050s, and (**f**) 2070s under RCP8.5 during the soybean growth period.

The climate tendency rate of ET_0 in the soybean growth period from 2021–2080 under RCP4.5 was 3.71–10.18 mm/(10 years). The climate tendency rates of ET_0 in 2021–2050, 2051–2080, and 2021–2080 were 12.65 mm/(10 years), 1.93 mm/(10 years), and 7.71 mm/(10 years), respectively (Figure 5a–c). Under RCP8.5, the climate tendency rate of ET_0 from 2021–2080 was 7.30–12.07 mm/(10 years), with an average of 9.55 mm/(10 years) (Figure 5d–f). All 26 sites passed the significance test at α = 0.001 under both RCP4.5 and RCP8.5.

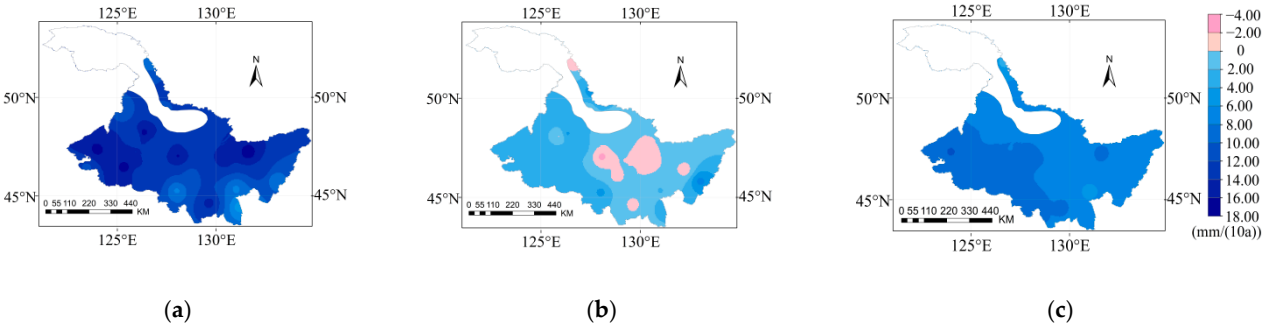

Figure 5. *Cont.*

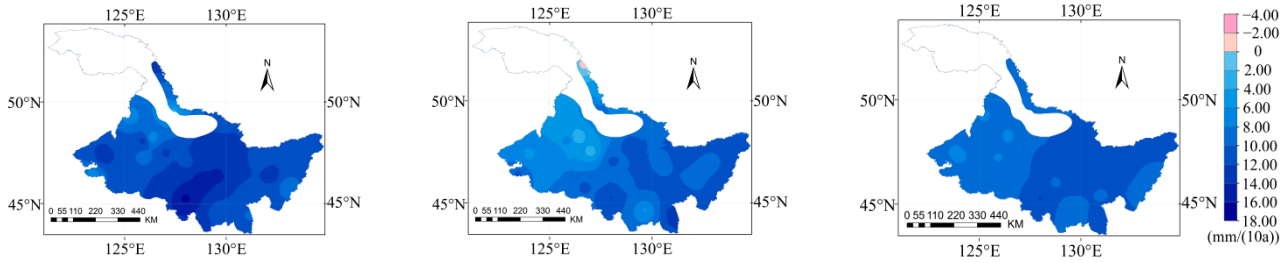

(**d**) (**e**) (**f**)

Figure 5. Climate tendency rates of ET_0 in the periods (**a**) 2021–2050, (**b**) 2051–2080, and (**c**) 2021–2080 under RCP4.5, and in the periods (**d**) 2021–2050, (**e**) 2051–2080, and (**f**) 2021–2080 under RCP8.5 during the soybean growth period.

3.3. Spatial and Temporal Variation of ET_c

The spatial distribution of ET_c and its climate tendency rate of soybean growth period for 2021–2080 under RCP4.5 and RCP8.5 are shown in Figures 6 and 7. Under RCP4.5, the ET_c values for 2021–2080 were 356.88–470.45 mm, with an average of 414.35 mm. Under RCP8.5, the average ET_c values for the 2030s, 2050s, and 2070s were 403.94, 423.39, and 436.07 mm, respectively. Under both RCP4.5 and RCP8.5, ET_c increased and then decreased from west to east in the study area.

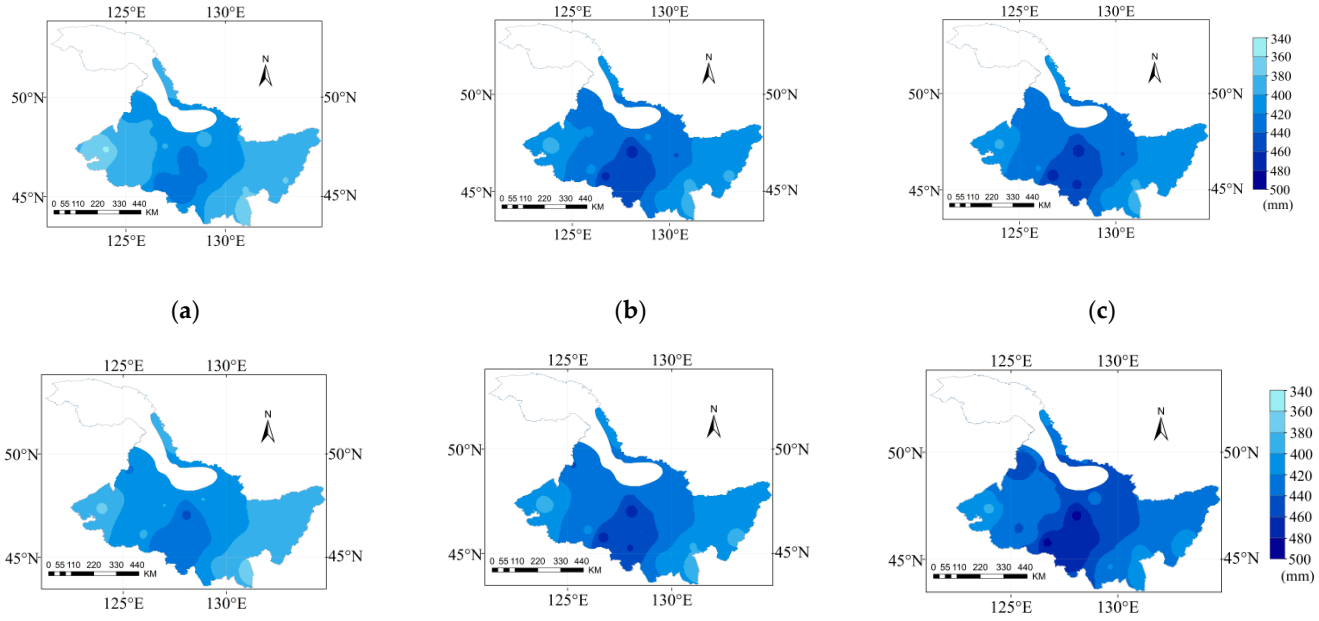

(**a**) (**b**) (**c**)

(**d**) (**e**) (**f**)

Figure 6. Spatial distribution of crop water requirement (ET_c) during the (**a**) 2030s, (**b**) 2050s, and (**c**) 2070s under RCP4.5, and during the (**d**) 2030s, (**e**) 2050s, and (**f**) 2070s under RCP8.5 during the soybean growth period.

As shown in Figure 7, the climate tendency rates of soybean ET_c for 2021–2080 were 2.92–8.11 mm/(10 years) and 4.08–9.39 mm/(10 years) under RCP4.5 and RCP8.5 with average values of 6.09 mm/(10 years) and 7.16 mm/(10 years), respectively. The ET_c climate tendency rate was higher in the western region than that in the eastern region under RCP4.5, whereas it was higher in the eastern region than that in the western region under RCP8.5. All 26 sites passed the significance test at $\alpha = 0.001$ under both RCP4.5 and

RCP8.5. Specifically, soybean ET_c in Yichun and Suifenhe increased at a rate of more than 11 mm/(10 years) under RCP8.5.

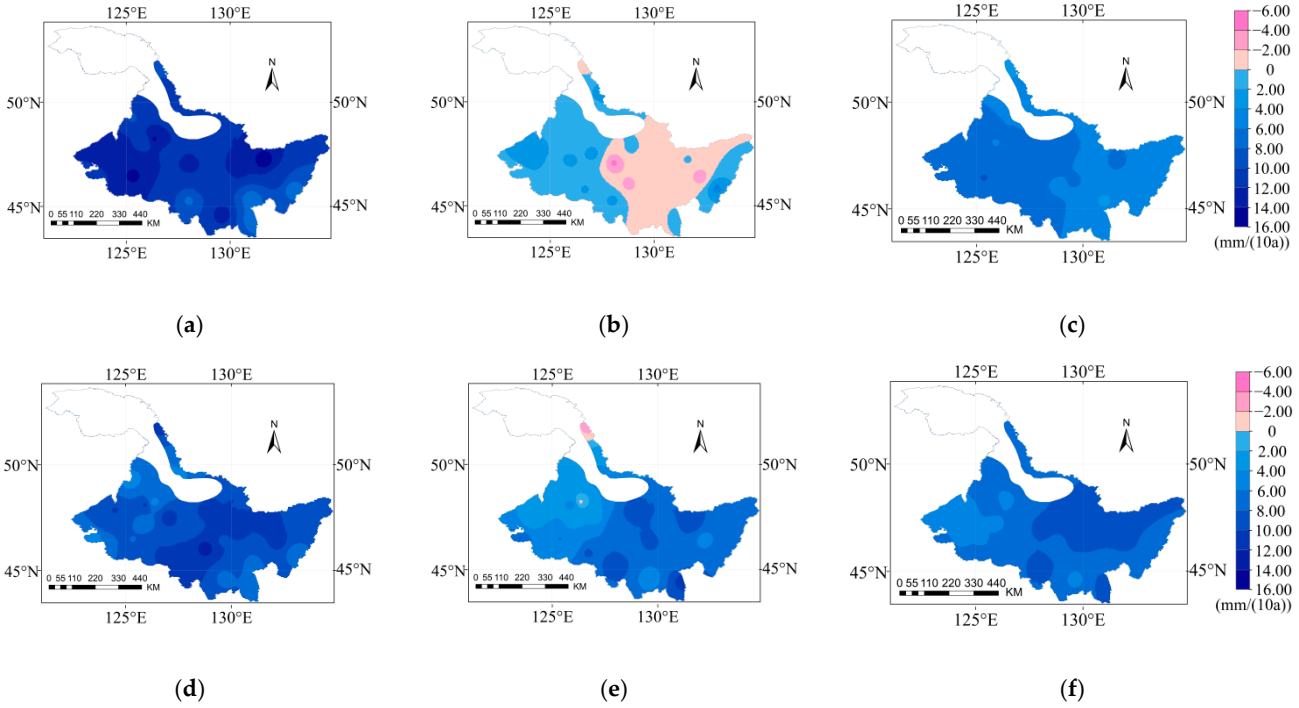

Figure 7. Climate tendency rates of ET_c in the periods (**a**) 2021–2050, (**b**) 2051–2080, and (**c**) 2021–2080 under RCP4.5, and in the periods (**d**) 2021–2050, (**e**) 2051–2080, and (**f**) 2021–2080 under RCP8.5 during the soybean growth period.

3.4. Spatial and Temporal Variation of P_e

The spatial distribution of P_e and its climate tendency rate under RCP4.5 and RCP8.5 during the soybean growth period for 2021–2080 are shown in Figure 8. Under RCP4.5 and RCP8.5, P_e values were 268.41–459.18 mm and 269.53–466.94 mm, with an average of 354.10 and 362.36 mm, respectively. Under RCP8.5, the greatest difference in P_e was 94.99 mm. Under RCP4.5 and RCP8.5, P_e first increased and then decreased from west to east; higher values were mainly distributed in Hailun and Tieli, with an average value greater than 370 mm, while lower values were mainly distributed in Tailai and Huma, with an average value lower than 340 mm.

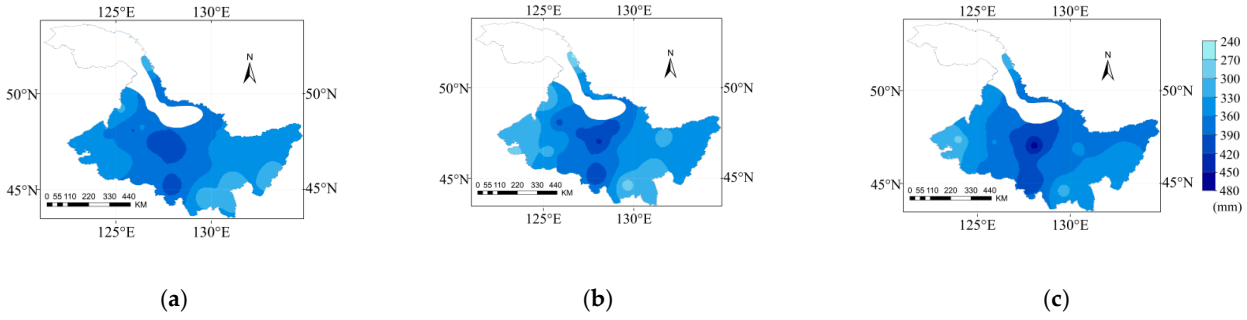

Figure 8. *Cont.*

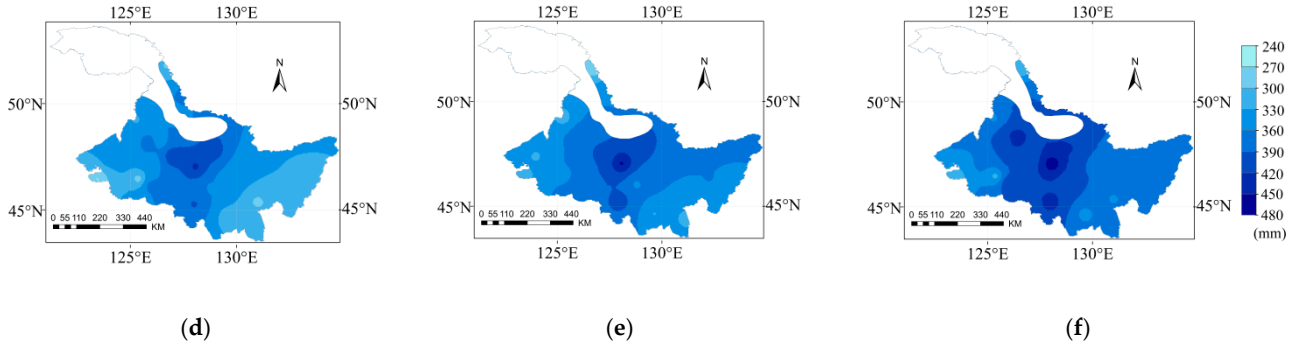

(**d**) (**e**) (**f**)

Figure 8. Spatial distribution of effective precipitation (P_e) during the (**a**) 2030s, (**b**) 2050s, and (**c**) 2070s under RCP4.5, and during the (**d**) 2030s, (**e**) 2050s, and (**f**) 2070s under RCP8.5 during the soybean growth period.

Under RCP4.5, the climate tendency rate of P_e during the soybean growth period from 2021–2080 was −10.81–10.11 mm/(10 years), and the average was 1.37 mm/(10 years) (Figure 9). A total of 16 sites showed an upward trend, while 10 sites showed a downward trend. Bei'an, Harbin, Jixi, Suifenhe, and Tieli passed the significance test at $\alpha = 0.05$, while Hulin, Keshan, and Suihua passed the significance test at $\alpha = 0.1$. Under RCP8.5, the climate tendency rate of Pe for 2021–2080 was −1.16–22.28 mm/(10 years), with an average value of 8.77 mm/(10 years). Bei'an, Mudanjiang, Suifenhe, Suihua, and Tonghe passed the significance test at $\alpha = 0.001$, while Baoqing, Fuyu, Fujin, and Mingshui passed the significance test at $\alpha = 0.05$.

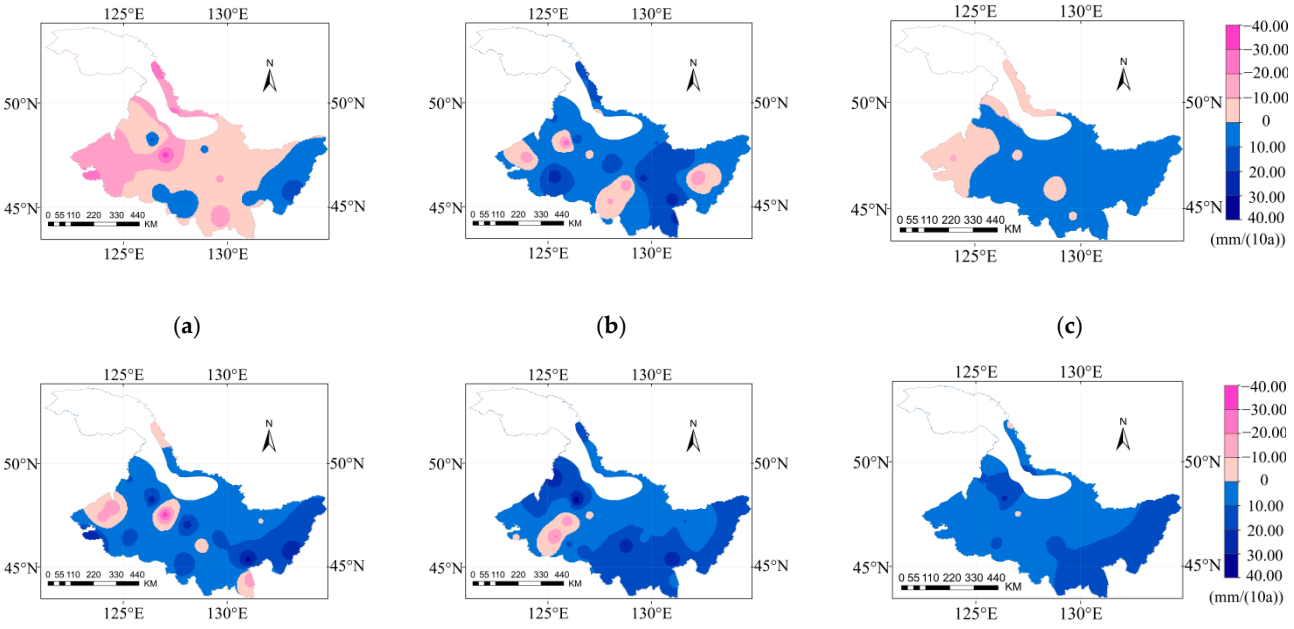

(**a**) (**b**) (**c**)

(**d**) (**e**) (**f**)

Figure 9. Climate tendency rates of P_e in the periods (**a**) 2021–2050, (**b**) 2051–2080, and (**c**) 2021–2080 under RCP4.5, and in the periods (**d**) 2021–2050, (**e**) 2051–2080, and (**f**) 2021–2080 under RCP8.5 during the soybean growth period.

3.5. Spatial and Temporal Variation of CD

The *CD* values during the soybean growth period under RCP4.5 and RCP8.5 from 2021–2080 are shown in Figure 10. Under RCP4.5 and RCP8.5, the *CD* for 2021–2080 ranged

from 0.66–0.95 and 0.66–0.96, with average values of 0.84 in both cases, showing a trend of first increasing and then decreasing in the study area.

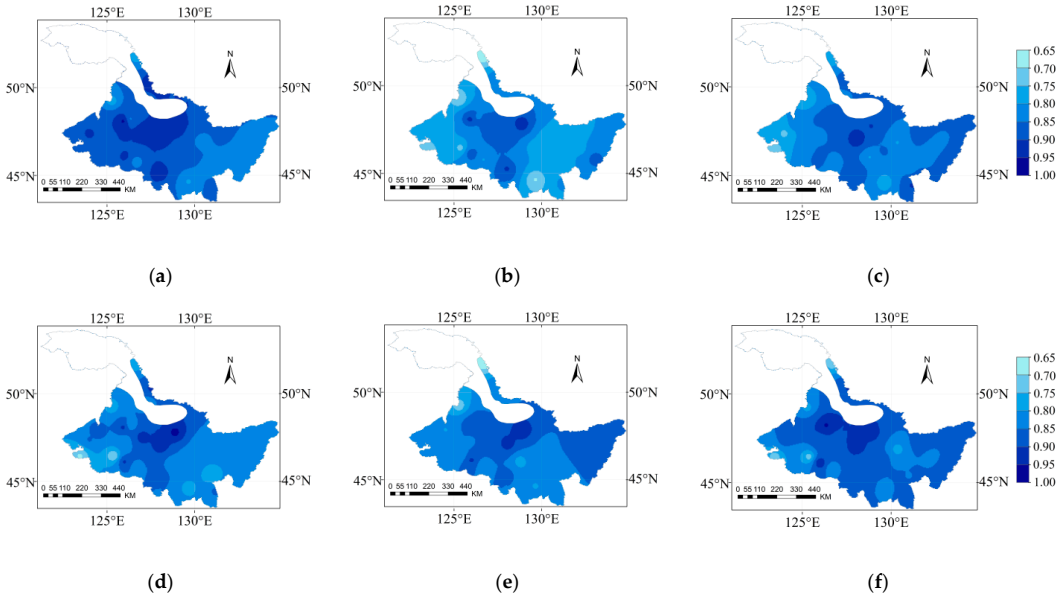

Figure 10. Spatial distribution of *CD* during the (**a**) 2030s, (**b**) 2050s, and (**c**) 2070s under RCP4.5, and during the (**d**) 2030s, (**e**) 2050s, and (**f**) 2070s under RCP8.5 during the soybean growth period.

The climate tendency rate of *CD* during the soybean growth period from 2021–2080 under the RCP4.5 was −0.036–0.014/(10 years), with an average value of −0.007/(10 years), showing an overall downward trend (Figure 11). Among them, Keshan and Qiqihar passed the significance test at $\alpha = 0.001$, while Fuyu and Shangzhi passed the significance test at $\alpha = 0.05$. However, under RCP8.5, the *CD* during the growth period of soybean ranged from −0.013 to 0.029/(10 years), with an average of 0.006/(10 years), showing an overall increasing trend. The climate tendency rates of *CD* at the 19 sites were greater than 0, among which Bei'an passed the significance test at $\alpha = 0.001$, while Mudanjiang and Tonghe passed the significance test at $\alpha = 0.05$.

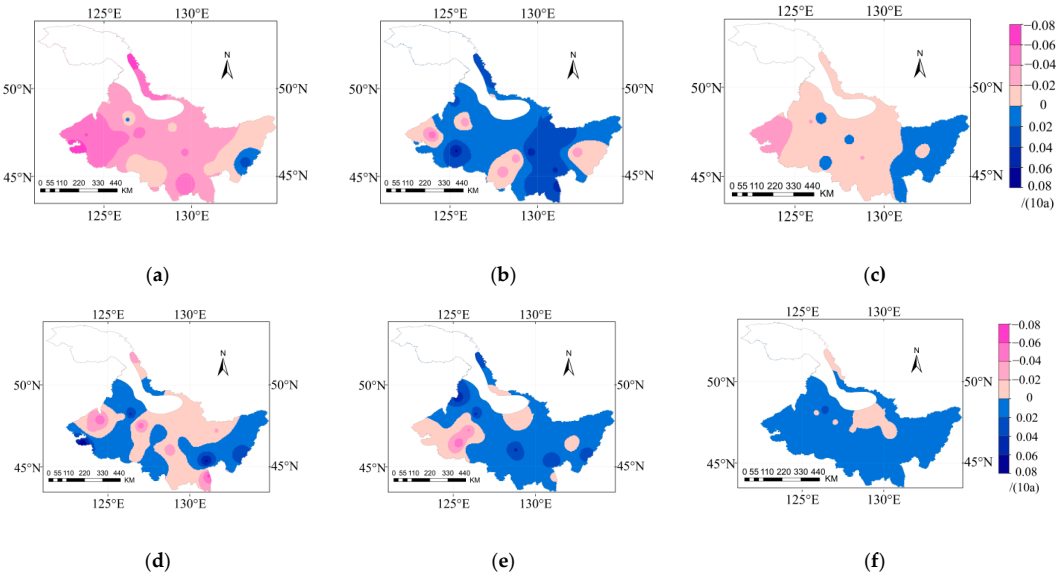

Figure 11. Climate tendency rates of *CD* in the periods (**a**) 2021–2050, (**b**) 2051–2080, and (**c**) 2021–2080 under RCP4.5, and in the periods (**d**) 2021–2050, (**e**) 2051–2080, and (**f**) 2021–2080 under RCP8.5 during the soybean growth period.

3.6. Spatial and Temporal Variation of I_r

The temporal and spatial distributions of I_r under RCP4.5 and RCP8.5 during the soybean growth period for 2021–2080 are shown in Figure 12. Under RCP4.5 and RCP8.5, the I_r values during 2021–2080 were 58.01–159.84 mm and 60.03–166.19 mm, with average values of 102.44 mm and 100.27 mm, respectively, which showed a trend of first decreasing and then increasing from west to east in the study area. Under RCP8.5, the greatest difference in I_r during the 2050s was as high as 43.32 mm, which was higher than that during the 2030s and 2050s (Figure 12d–f).

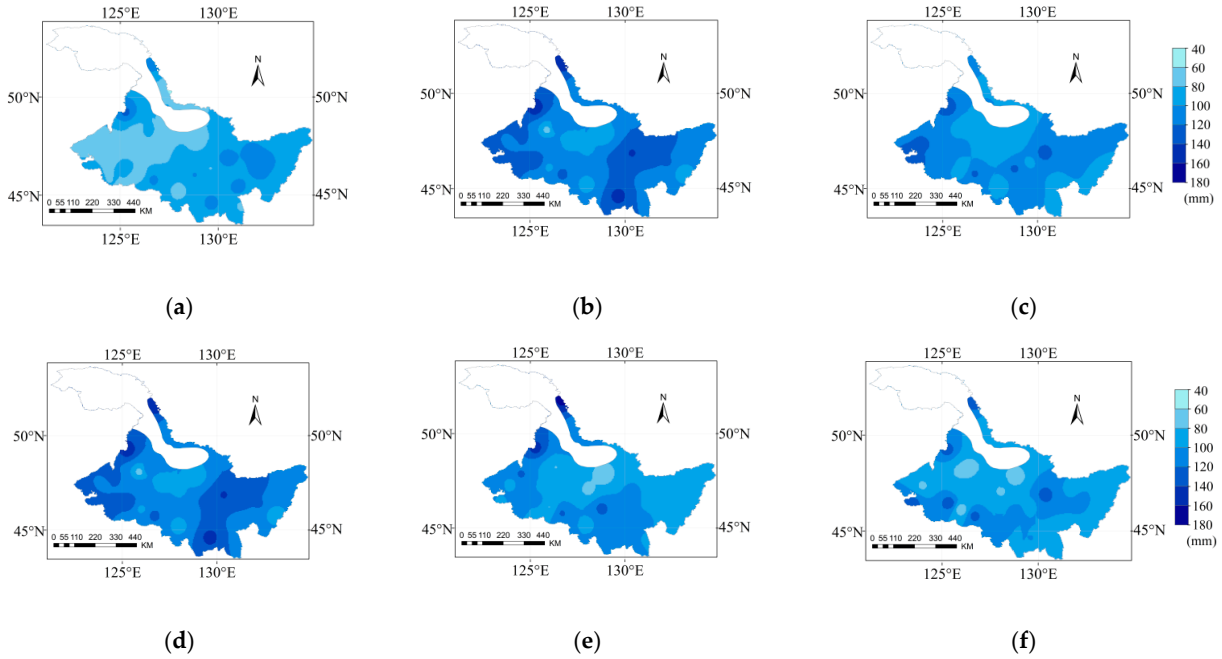

Figure 12. Spatial distribution of irrigation water requirement (I_r) during the (**a**) 2030s, (**b**) 2050s, and (**c**) 2070s under RCP4.5, and during the (**d**) 2030s, (**e**) 2050s, and (**f**) 2070s under RCP8.5 during the soybean growth period.

The average climate tendency rates of I_r during the growth period of soybean under RCP4.5 in 2021–2051, 2051–2080, and 2021–2080 were 14.88, −5.92, and 3.73 mm/(10 years), respectively (Figure 13). Among the 26 sites, Qiqihar increased at a significance of $\alpha = 0.001$. Under RCP8.5, the average climate tendency rate of I_r for 2021–2080 was −0.067 mm/(10 years). I_r showed an overall downward trend (Figure 13d–f). During the whole period of the study, the climate tendency rates of I_r in 16 sites were negative, accounting for 61.54% of the total site number, among which, Bei'an decreased at a significance of $\alpha = 0.001$.

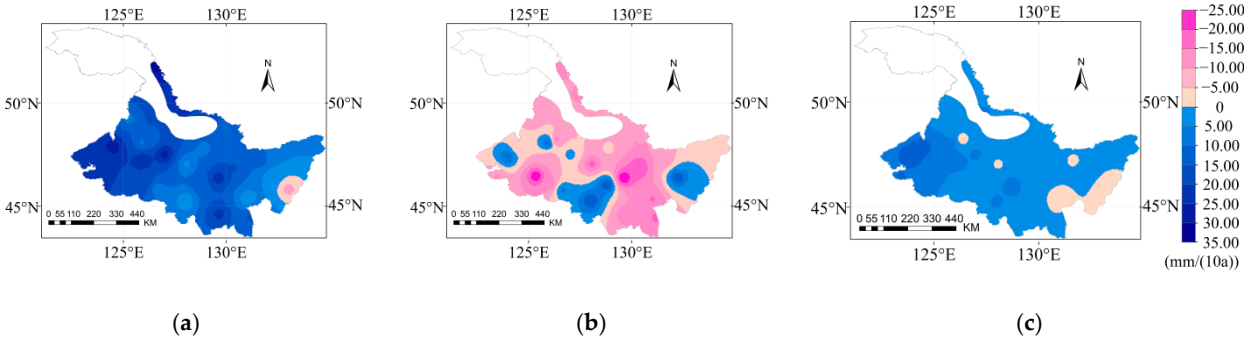

Figure 13. *Cont.*

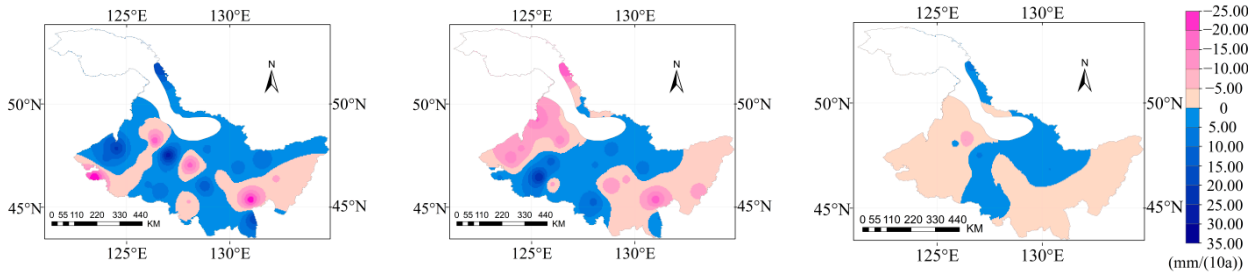

(**d**) (**e**) (**f**)

Figure 13. Climate tendency rates of I_r in the periods (**a**) 2021–2050, (**b**) 2051–2080, and (**c**) 2021–2080 under RCP4.5, and in the periods (**d**) 2021–2050, (**e**) 2051–2080, and (**f**) 2021–2080 under RCP8.5 during the soybean growth period.

3.7. Effect of Climate Change on Water Supply and Requirement

Under RCP4.5 and RCP8.5, soybean ET_c was significantly positively correlated with T_{max} and *Rad* and negatively correlated with *RH* (Table 2). Under RCP8.5, P_e was significantly negatively correlated with T_{max} and *Rad*, significantly positively correlated with T_{min}, and weakly correlated with *RH*. Under RCP4.5, I_r was significantly positively correlated with average T_{min}, T_{max}, and *Rad*, and significantly negatively correlated with average *RH*. The effects of meteorological factors on soybean ET_c in the study area under RCP4.5 and RCP8.5 for 2021–2080 and the relationships among P_e, ET_c, and I_r are shown in Figure 14. Under RCP4.5 and RCP8.5, soybean ET_c was significantly correlated with average T_{min}, T_{max}, *RH*, and *Rad*. The increase in temperature and *Rad* led to an increase in ET_0, further increasing ET_c (Table 2). The correlation coefficient between ET_c and *Rad* was greater than that of T_{max}, indicating that the increasing soybean ET_c was most influenced by *Rad*, followed by T_{max}. The *CD* tended to decrease and then increase under RCP4.5; however, it tended to increase under RCP8.5 from the 2030s to 2070s. Under RCP4.5, ET_c increased by 29.45 and 5.55 mm in the 2030s–2050s and 2050s–2070s, respectively, while P_e decreased by 12.21 mm in 2030s–2050s and then increased by 16.78 mm in 2050s–2080s. The combined effects of ET_c and P_e led to a change in I_r, which first increased by 31.01 mm and then decreased by 13.65 mm from the 2030s to 2070s (Figure 14).

Table 2. Correlation analysis among ET_0, ET_c, P_e, I_r, and meteorological factors during the soybean growth period.

Items	Scenarios	Periods	T_{min}	T_{max}	*RH*	*Rad*
ET_0	RCP4.5	2030s	−0.176	−0.522 *	−0.769 **	0.790 **
		2050s	0.087	0.779 **	−0.727 **	0.892 **
		2070s	0.057	0.926 **	−0.863 **	0.912 **
		2030s–2070s	0.898 **	0.982 **	−0.831 **	0.908 **
	RCP8.5	2030s	−0.059	0.405	−0.450 *	0.508 *
		2050s	−0.386	0.852 **	−0.924 **	0.963 **
		2070s	−0.473 *	0.854 **	−0.885 **	0.929 **
		2030s–2070s	0.971 **	0.991 **	−0.226	0.697 **
ET_c	RCP4.5	2030s	−0.291	0.548 *	−0.826 **	0.849 **
		2050s	−0.089	0.598 **	−0.780 **	0.892 **
		2070s	−0.091	0.790 **	−0.798 *	0.823 **
		2030s–2070s	0.855 **	0.960 **	−0.873 **	0.939 **
	RCP8.5	2030s	−0.214	0.298	−0.595 **	0.649 **
		2050s	−0.395	0.739 **	−0.820 **	0.884 **
		2070s	−0.489 *	0.726 **	−0.841 **	0.890 **
		2030s–2070s	0.962 **	0.984 **	−0.851 **	0.716 **

Table 2. *Cont.*

Items	Scenarios	Periods	T_{min}	T_{max}	*RH*	*Rad*
P_e	RCP4.5	2030s	−0.240	−0.338	0.140	−0.114
		2050s	0.390	0.025	−0.487	−0.436
		2070s	−0.149	−0.223	0.255	−0.208
		2030s–2070s	0.167	−0.021	0.387 **	−0.306 *
	RCP8.5	2030s	0.206	0.081	0.136	−0.142
		2050s	0.099	−0.344	0.375	−0.339
		2070s	0.482 *	−0.001	−0.248	−0.306
		2030s–2070s	0.810 **	−0.793 **	−0.110	−0.324 *
I_r	RCP4.5	2030s	0.152	0.287	−0.184	0.167
		2050s	−0.283	0.291	−0.698 **	0.693 **
		2070s	−0.016	0.381	−0.434	0.419
		2030s–2070s	0.409 **	0.590 **	−0.841 **	0.824 **
	RCP8.5	2030s	−0.232	−0.078	−0.209	0.209
		2050s	−0.231	0.434	−0.547 *	0.550 *
		2070s	−0.531 *	0.268	−0.489 *	0.582 **
		2030s–2070s	−0.140	0.094	−0.400 **	0.283 *

Note: * significant correlation at the 0.05 level; ** significant correlation at the 0.01 level.

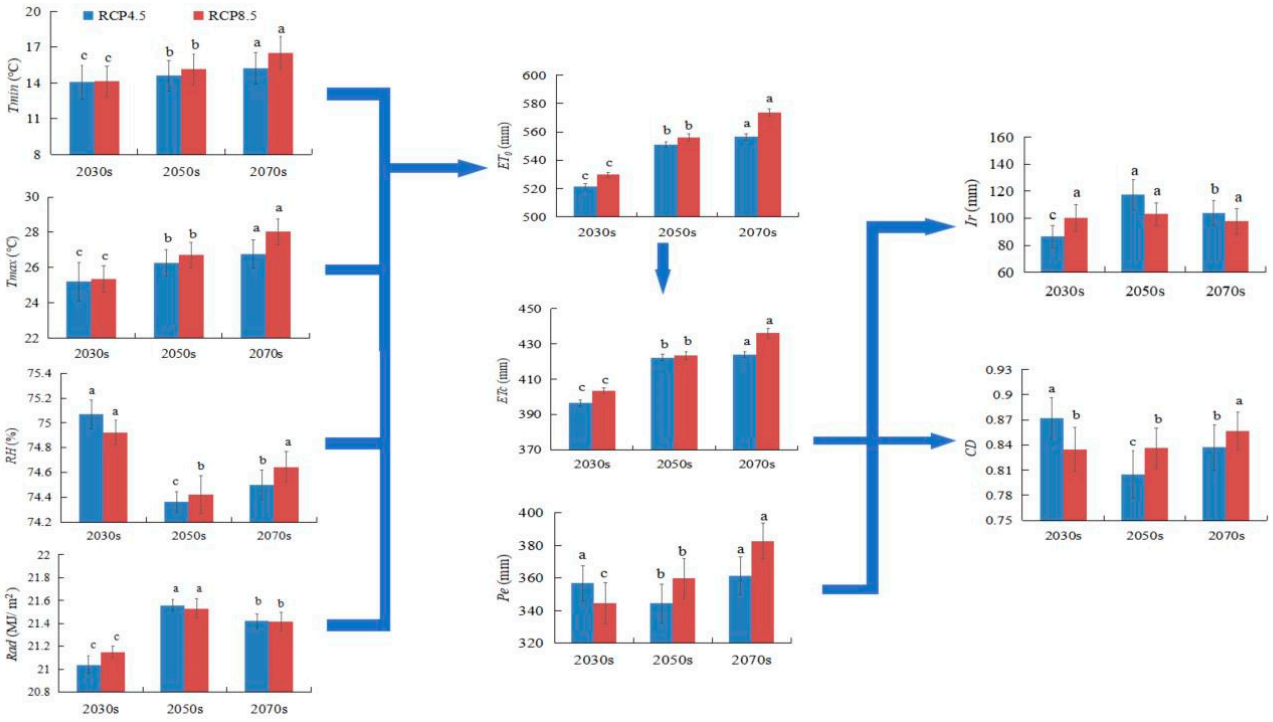

Figure 14. Effects of changes in meteorological factors on soybean ET_c and the relationships among P_e, ET_c, and I_r under RCP4.5 and RCP8.5 for 2021–2080. Bars marked with different lowercase letters indicate significant differences between groups ($p < 0.05$), while those marked with the same lowercase letters indicate insignificant differences between groups ($p > 0.05$).

4. Discussion

4.1. Soybean ET_c and Meteorological Factors

Soybean ET_c showed an increasing trend from the 2030s to 2070s under RCP4.5 and RCP8.5 in Heilongjiang Province of China in this study. An upward trend in ET_c was also observed in previous studies involving different crops under future climate change, including maize in Zimbabwe in the 2020s, 2050s, and 2090s [13], sugarcane in Pakistan in the 2020s, 2050s, and 2080s [45], rice in Kunshan in the 2020s–2080s [7], wheat, maize, and

gram in India in the 2020s–2080s [28], wheat in three provinces of northeast China in the 2040s, 2070s, and 2100s [23], and summer maize in Huang-Huai-Hai Plain in 2016–2050 [46].

In the 60 year time series under RCP4.5 and RCP8.5 covered in this study, T_{min}, T_{max}, *Rad*, and *RH* were all strongly related to the increase in ET_c. Yang et al. (2021) found that *Rad*, wind speed, and *P* had the strongest linear correlations with cotton ET_c, with correlation coefficients of 0.410–0.789, 0.361–0.676, and −0.215–−0.410, for 1965–2016 in NCP, respectively. The correlation of ET_c with *RH* and average temperature were weak, in the range of −0.189–−0.047 and −0.102–0.015, respectively [16]. In contrast, under RCP4.5 and RCP8.5, the decline rate of *RH* climate tendency rate in Heilongjiang Province was almost twice that of the NCP. The decreased *RH* in the air increased the evaporation rate, thus increasing ET_c [47]. Nageen reported an increasing trend in ET_c for sugarcane as well, which was due to the forecasted temperature rise in the future Pakistan region, while the increased P_e could not compensate for the increased ET_c [45]. In addition, this study found that the increase in sunshine hours provided more radiation and light energy to the soybean [48], thus promoting the opening of stomata for plant transpiration and leading to an increase in transpiration [49]; accordingly, ET_c showed an increasing trend. Li et al. [46] reported that the temperature would continue to rise in the future in the Huang-Huai-Hai Plain, while the summer maize evaporation would increase, resulting in increased ET_c. However, this study focused more on the impact of the combined effects of T_{min}, T_{max}, *RH*, and *Rad* meteorological factors on the increase in ET_c in soybean.

4.2. Soybean ET_c, P_e, and I_r

In this study, the annual average ET_c for the soybean growing season under RCP4.5 and RCP8.5 for 2021–2080 was higher than that of soybean in Heilongjiang Province for 1966–2015 reported by Li et al. [30]. The higher ET_c indicated soybean in this study area may suggest the need for more water due to the increase in evapotranspiration derived from future climate conditions [50]. Oludare et al. (2020) reported that the average temperature and *Rad* increased, while soybean ET_c increased slightly under RCP4.5 and RCP8.5 for 2021–2099 in the Ogun-Ona River Basin, Nigeria [50]. Similar to the results of this study, the ET_c of soybean in different regions of the world also increased with the same trend of meteorological factors.

Under RCP4.5 and RCP8.5, the P_e and I_r of soybean were higher than reported by Li et al. [30]. Although a small increase in P_e was predicted in the future, more I_r was still needed, which probably increased the pressure on agricultural water, as well as drought frequency [51]. The highest ET_c and P_e under RCP4.5 and RCP8.5 in this study were distributed in the south; however, Li et al. (2020) reported that the highest ET_c and P_e were in the west [34]. Due to the increase in T_{min}, T_{max}, and *Rad* in the southern region and the decrease in *RH*, higher ET_c is expected in the future. Moreover, in the historical period, Li et al. [34] did not consider the influence of *Rad* on ET_c. In addition, ET_c is also affected by the plant itself, such as plant canopy structure and plant physiology [52]. Under RCP4.5, the climate tendency rate of ET_c was much greater in the west than that in the east; however, under RCP8.5, the climate tendency rate of ET_c showed an opposite spatial distribution trend, which differed from the results of Hu et al. [37]. This might be due to the higher values of *Rad* under RCP8.5, resulting in an increase in the climate tendency rate of ET_c in the east. On the other hand, the meteorological factors came from different meteorological stations and time series [53]. Under future climate change, their increasing or decreasing trends and magnitudes are also very different from the past [54]. This study provides long-term information for soybean water and irrigation requirements in Heilongjiang Province of China under future climate change [55].

4.3. Uncertainties and Limitations of the Study

This study indicated that there was a strong relationship among temperature, P_e variability, ET_c, and I_r under climate change. Two limitations should be taken into account in this study. Firstly, due to political and socioeconomic factors, regional climate

programs are unable to accurately predict the path of future greenhouse gas emissions [56]. We only considered the RCP4.5 and RCP8.5, in which the concentration of CO_2 is fixed; however, in fact, the concentration of CO_2 varies with time [2]. In addition, the "Special Report on Emission Scenarios" (SRES) also proposed that two other emission scenarios, A1 (emphasizing economic development) and B2 (emphasizing sustainable development), can also predict the future climate [23]. However, anthropogenic-based climate change scenarios are one-sided scenarios. Under the actual climate in the future, the biological and agricultural technological progress of soybean planting will certainly change to reduce the impact of climate change. Secondly, we adjusted the parameters of the CROPWAT crop model for Heilongjiang Province, but there were still some uncertainties in the simulation parameters. For example, K_c and crop phenology are expected to change under future climatic change [57]. Therefore, changes in all meteorological factors caused by global warming and the uncertainties and limitations of the model should be deeply considered in further study.

5. Conclusions

In 2021–2080, T_{min}, T_{max}, and *Rad* increased while *RH* decreased under RCP4.5 and RCP8.5. In particular, the climate tendency rates for T_{min}, T_{max}, and *Rad* were higher under RCP8.5. There was little difference in the climate tendency rate of *RH* between RCP4.5 and RCP8.5. Affected by the changes in climate factors in the future, the ET_0, ET_c, and P_e during soybean growth period in Heilongjiang Province showed an upward trend under RCP4.5 and RCP8.5. The climate tendency rates of annual ET_c were 6.09 mm/(10 years) and 7.16 mm/(10 years), respectively. The climate tendency rate of annual I_r was 3.73 mm/(10 years) under RCP 4.5, while it was −0.067 mm/(10 years) under RCP 8.5. The results showed that the soybean in whole Heilongjiang province would face water shortage stress in the future, especially in the central and western regions. There would be more P and less ET_c in the eastern region. Therefore, we should appropriately adjust the crop structure, change the planting system, and recommend increasing the soybean planting area in the eastern Heilongjiang Province. This study can guide future irrigation system planning and management policy in Heilongjiang Province.

Author Contributions: Conceptualization, T.N. and N.L.; methodology, T.N. and N.L.; validation, Y.T., Y.J. and Z.Z.; formal analysis, N.L. and T.N.; writing—original draft preparation, N.L. and T.N.; writing—review and editing, T.W., Z.Z., P.C., T.L., L.M. and K.C.; visualization, N.L., Y.T., D.L. and T.W.; supervision, T.N.; project administration, T.N.; funding acquisition, T.N. All authors have read and agreed to the published version of the manuscript.

Funding: This work was fund by Basic Scientific Research Fund of Heilongjiang Provincial Universities (grant number: 2021-KYYWF-0019), the Opening Project of Key Laboratory of Efficient Use of Agricultural Water Resources, Ministry of Agriculture and Rural Affairs of the People's Republic of China in Northeast Agricultural University (grant number: AWR2021002), and the National Natural Science Foundation Project of China (grant number: 51779046).

Institutional Review Board Statement: Not applicable.

Informed Consent Statement: Not applicable.

Data Availability Statement: The data presented in this study are available on request from the corresponding author.

Acknowledgments: We thank the Chinese meteorological data sharing service (http://data.cma.cn, accessed on 22 May 2022) for providing the meteorological data. We thank all the members in the Lab of the Pumping, Hydraulic Teaching, and Experimental Center of Heilongjiang University. Lastly, we thank the anonymous reviewers and the editor for their suggestions, which substantially improved the manuscript.

Conflicts of Interest: The authors declare no conflict of interest.

References

1. Chen, Y.Y. Impact of climate change on grain production in China. *Chin. Agric. Sci. Bull.* **2021**, *12*, 51–57. (In Chinese)
2. Intergovernmental Panel on Climate Change (IPCC). *Global Warming of 1.5 °C; Impacts of 1.5 °C of Global Warming on Natural and Human Systems. Contribution of Working Group I to the Sixth Assessment Report of the Intergovernmental Panel on Climate Change*; Intergovernmental Panel on Climate Change (IPCC): Geneva, Switzerland, 2018; *in press*.
3. Wang, T.; Du, C.; Nie, T.; Sun, Z.; Zhu, S.; Feng, C.; Dai, C.; Chu, L.; Liu, Y.; Liang, Q. Spatiotemporal analysis of maize water requirement in the Heilongjiang Province of China during 1960–2015. *Water* **2020**, *12*, 2472. [CrossRef]
4. Tang, C.X. Influence of rainfall weather on agricultural production and countermeasures. *Agric. Dev. Equip.* **2019**, *10*, 68–69. (In Chinese)
5. Bouras, E.; Jarlan, L.; Khabba, S.; Er-Raki, S.; Dezetter, A.; Sghir, F.; Tramblay, Y. Assessing the impact of global climate changes on irrigated wheat yields and water requirements in a semi-arid environment of Morocco. *Sci. Rep.* **2019**, *9*, 19142. [CrossRef]
6. Ding, Y.; Wang, W.; Zhuang, Q.; Luo, Y. Adaptation of paddy rice in China to climate change: The effects of shifting sowing date on yield and irrigation water requirement. *Agric. Water Manag.* **2020**, *228*, 105890. [CrossRef]
7. Wang, W.G.; Sun, F.Z.; Peng, S.Z.; Xu, J.Z.; Luo, Y.F.; Jiao, X.Y. Simulation of response of rice irrigation water demand to climate change. *Trans. Chin. Soc. Agric. Eng.* **2013**, *14*, 90–98. (In Chinese)
8. Acharjee, T.K.; Ludwig, F.; van Halsema, G.; Hellegers, P.; Supit, I. Future changes in water requirements of Boro rice in the face of climate change in North-West Bangladesh. *Agric. Water Manag.* **2017**, *194*, 172–183. [CrossRef]
9. Cheshmberah, F.; Zolfaghari, A.A. The Effect of Climate Change on Future Reference Evapotranspiration in Different Climatic Zones of Iran. *Pure Appl. Geophys.* **2019**, *176*, 3649–3664. [CrossRef]
10. Ti, J.; Yang, Y.; Yin, X.; Liang, J.; Pu, L.; Jiang, Y.; Wen, X.; Chen, F. Spatio-Temporal Analysis of Meteorological Elements in the North China District of China during 1960–2015. *Water* **2018**, *10*, 789. [CrossRef]
11. Nie, T.; Tang, Y.; Jiao, Y.; Li, N.; Wang, T.; Du, C.; Zhang, Z.; Chen, P.; Li, T.; Sun, Z.; et al. Effects of Irrigation Schedules on Maize Yield and Water Use Efficiency under Future Climate Scenarios in Heilongjiang Province Based on the AquaCrop Model. *Agronomy* **2022**, *12*, 810. [CrossRef]
12. Lyu, J.; He, Q.-Y.; Chen, Q.-W.; Cheng, R.-R.; Li, G.; Otsuki, K.; Yamanaka, N.; Du, S. Distinct transpiration characteristics of black locust plantations acclimated to semiarid and subhumid sites in the Loess Plateau, China. *Agric. Water Manag.* **2022**, *262*, 107402. [CrossRef]
13. Nkomozepi, T.; Chung, S.-O. Assessing the trends and uncertainty of maize net irrigation water requirement estimated from climate change projections for Zimbabwe. *Agric. Water Manag.* **2012**, *111*, 60–67. [CrossRef]
14. Xiao, D.; Liu, D.L.; Wang, B.; Feng, P.; Bai, H.; Tang, J. Climate change impact on yields and water use of wheat and maize in the North China Plain under future climate change scenarios. *Agric. Water Manag.* **2020**, *238*, 106238. [CrossRef]
15. Yang, X.; Jin, X.; Chu, Q.; Pacenka, S.; Steenhuis, T.S. Impact of climate variation from 1965 to 2016 on cotton water requirements in North China Plain. *Agric. Water Manag.* **2021**, *243*, 106502. [CrossRef]
16. Chen, D.W. Advances in Prediction and Calculation of Crop Water Demand. *Hydro Sci. Cold Zone Eng.* **2021**, *4*, 171–174. (In Chinese)
17. Wang, Y.; Shao, X.H.; Li, Y.H. Research progress on real-time prediction method of reference crop water requirement. *J. Anhui Agric. Sci.* **2008**, *36*, 13919–13920. (In Chinese) [CrossRef]
18. Tavakoli, A.R.; Moghadam, M.M.; Sepaskhah, A.R. Evaluation of the AquaCrop model for barley production under deficit irrigation and rainfed condition in Iran. *Agric. Water Manag.* **2015**, *161*, 136–146. [CrossRef]
19. FAO. *OECD-FAO Agricultural Outlook*; OECD Publishing, Food and Agriculture Organization of the United Nations: Rome, Italy, 2009; pp. 2011–2020.
20. Lu, X.P.; Duan, S.Q.; Ma, X.Y.; Bai, S.M. Comparative Study on Calculation of Maize Water Demand by Single and Double Crop Coefficient Method. *Water Sav. Irrig.* **2012**, *11*, 18–21. (In Chinese)
21. Zhang, L.; Tan, F.; Li, S.; Huo, Z. Potential dynamic of irrigation water requirement for rice across Northeast China. *Theor. Appl. Climatol.* **2020**, *142*, 1283–1293. [CrossRef]
22. Wu, J.B.; Ma, Y.F.; Zheng, H.X.; Cao, X.S. Estimation of maize evapotranspiration in semi-arid region based on modified crop coefficient model. *J. Water Resour. Archit. Eng.* **2020**, *18*, 25–29. (In Chinese)
23. Zhang, J.P.; Wang, C.Y.; Yang, X.G.; Zhao, Y.X.; Liu, Z.J.; Wang, J.; Chen, Y.Y. Prediction of the impact of future climate change on maize water demand in Northeast China. *Trans. Chin. Soc. Agric. Eng.* **2009**, *25*, 50–55. (In Chinese)
24. Nie, T.Z.; Zhang, Z.X.; Qi, Z.J.; Chen, P.; Lin, Y.Y.; Sun, Z.Y. Spatial-temporal distribution characteristics of rice water demand in Heilongjiang Province from 1960 to 2015. *Trans. Chin. Soc. Agric. Mach.* **2019**, *50*, 279–290. (In Chinese)
25. Jin, X. Application of Penman Formula in Crop Water Demand Calculation. *Jianghuai Water Resour. Sci. Technol.* **2018**, *1*, 28–30. (In Chinese)
26. Awal, R.; Fares, A.; Bayabil, H. Assessing Potential Climate Change Impacts on Irrigation Requirements of Major Crops in the Brazos Headwaters Basin, Texas. *Water* **2018**, *10*, 1610. [CrossRef]
27. Hong, E.-M.; Nam, W.-H.; Choi, J.-Y.; Pachepsky, Y.A. Projected irrigation requirements for upland crops using soil moisture model under climate change in South Korea. *Agric. Water Manag.* **2016**, *165*, 163–180. [CrossRef]
28. Hossain, M.B.; Roy, D.; Maniruzzaman, M.; Biswas, J.C.; Naher, U.A.; Haque, M.M.; Kalra, N. Response of crop water requirement and yield of irrigated rice to elevated temperature in Bangladesh. *Int. J. Agron.* **2021**, *2021*, 9963201. [CrossRef]

29. Sunil, A.; Deepthi, B.; Mirajkar, A.B.; Adarsh, S. Modeling future irrigation water demands in the context of climate change: A case study of Jayakwadi command area, India. *Model. Earth Syst. Environ.* **2021**, *7*, 1963–1977. [CrossRef]
30. Goodarzi, M.; Abedi-Koupai, J.; Heidarpour, M. Investigating Impacts of Climate Change on Irrigation Water Demands and Its Resulting Consequences on Groundwater Using CMIP5 Models. *GroundWater* **2019**, *57*, 259–268. [CrossRef]
31. Chen, P.; Nie, T.; Chen, S.; Zhang, Z.; Qi, Z.; Liu, W. Recovery efficiency and loss of 15N-labelled urea in a rice-soil system under water saving irrigation in the Songnen Plain of Northeast China. *Agric. Water Manag.* **2019**, *222*, 139–153. [CrossRef]
32. Chen, P.; Xu, J.; Zhang, Z.; Wang, K.; Li, T.; Wei, Q.; Li, Y. Carbon pathways in aggregates and density fractions in Mollisols under water and straw management: Evidence from 13C natural abundance. *Soil Biol. Biochem.* **2022**, *169*, 108684. [CrossRef]
33. Heilongjiang Provincial People's Government. *Heilongjiang Yearbook*; Editorial Department: Harbin, China, 2020; pp. 244–245. ISSN 1008-0791.
34. Li, J.Y.; Wang, X.L.; Wang, Z.B.; Nie, T.Z. Spatial and Temporal Distribution of Soybean Water Demand and Drought in Heilongjiang Province in Recent 50 Years. *Trans. Chin. Soc. Agric. Mach.* **2020**, *51*, 223–237. (In Chinese)
35. Hu, H.J.; Wang, M.; Yin, X.G.; Jiang, Y.L.; Wen, X.Y.; Chen, F. Analysis on Temporal and Spatial Variation Characteristics of Soybean Water Demand in Northeast Agricultural Region under Climate Change. *Zhongguo Nongye Daxue Xuebao* **2017**, *22*, 21–31. (In Chinese)
36. Accumulated Temperature Zone of Crop Varieties in Heilongjiang Province. Available online: http://www.hljagri.gov.cn/ (accessed on 2 September 2020).
37. Area Layout Planning of High-Quality and High-yield Main Food Crops in Heilongjiang Province in 2015. Available online: http://dszz.hljagri.gov.cn/tjxxw/jrtj/tzgg/201501/ (accessed on 2 September 2020).
38. Smith, M. *CROPWAT: A Computer Program for Irrigation Planning and Management*; FAO: Rome, Italy, 1992.
39. FAO. *Crop Evapotranspiration for Computing Crop Water Requirement*; FAO Irrigation & Drainage Paper: Rome, Italy, 1998; p. 56.
40. Gocic, M.; Trajkovic, S. Analysis of changes in meteorological variables using Mann-Kendall and Sen's slope estimator statistical tests in Serbia. *Glob. Planet. Change* **2013**, *100*, 172–182. [CrossRef]
41. Bahmani, S.; Bajic, I.V.; HajShirmohammadi, A. Joint Decoding of Unequally Protected JPEG2000 Bitstreams and Reed-Solomon Codes. *IEEE Trans. Image Process.* **2010**, *19*, 2693–2704. [CrossRef] [PubMed]
42. Tsakmakis, I.D.; Zoidou, M.; Gikas, G.D.; Sylaios, G.K. Impact of Irrigation Technologies and Strategies on Cotton Water Footprint Using AquaCrop and CROPWAT Models. *Environ. Process.* **2018**, *5*, S181–S199. [CrossRef]
43. Dubrau, A.W.; Hendren, L.J. Taming MATLAB. *Acm Sigplan Notice* **2012**, *47*, 503–522. [CrossRef]
44. Xiao, Z.L. A comparative study of using MATLAB and SPSS software to solve regression analysis. *Shanxi Youth* **2016**, *18*, 58–59. (In Chinese)
45. Farooq, N.; Gheewala, S.H. Assessing the impact of climate change on sugarcane and adaptation actions in Pakistan. *Acta Geophys.* **2020**, *68*, 1489–1503. [CrossRef]
46. Li, Y.; Qu, H.J.; Su, W.Y.; Gao, Z.P.; Wu, J.M. Response of Crop Irrigation Water Demand in Typical Area of Huanghuai Plain under HadGEM2-ES Climate Model. *Water Resour. Power* **2017**, *35*, 119–122. (In Chinese)
47. Jalota, S.K.; Sood, A.; Chahal, G.B.S.; Choudhury, B.U. Crop water productivity of cotton (*Gossypium hirsutum* L.)–wheat (*Triticum aestivum* L.) system as influenced by deficit irrigation, soil texture and precipitation. *Agric. Water Manag.* **2006**, *84*, 137–146. [CrossRef]
48. Liu, B.; Zhang, D.; Zhang, H.; Asseng, S.; Yin, T.; Qiu, X.; Ye, Z.; Liu, L.; Tang, L.; Cao, W.; et al. Separating the impacts of heat stress events from rising mean temperatures on winter wheat yield of China. *Environ. Res. Lett.* **2021**, *16*, 124035. [CrossRef]
49. Paul, M.; Dangol, S.; Kholodovsky, V.; Sapkota, A.R.; Negahban-Azar, M.; Lansing, S.L. Modeling the Impacts of Climate Change on Crop Yield and Irrigation in the Monocacy River Watershed, USA. *Climate* **2020**, *8*, 139. [CrossRef]
50. Durodola, O.S.; Mourad, K.A. Modelling the Impacts of Climate Change on Soybeans Water Use and Yields in Ogun-Ona River Basin, Nigeria. *Agriculture* **2020**, *10*, 593. [CrossRef]
51. Soares, D.; Rolim, J.; Fradinho, M.J.; Paço, T.A.D. Climate Change Impacts on Irrigation Requirements of Preserved Forage for Horses under Mediterranean Conditions. *Agronomy* **2020**, *10*, 1758. [CrossRef]
52. Luo, X.; Xia, J.; Yang, H. Modeling water requirements of major crops and their responses to climate change in the North China Plain. *Environ. Earth Sci.* **2015**, *74*, 3531–3541. [CrossRef]
53. Gao, J.; Yang, X.; Zheng, B.; Liu, Z.; Zhao, J.; Sun, S.; Li, K.; Dong, C. Effects of climate change on the extension of the potential double cropping region and crop water requirements in Northern China. *Agric. For. Meteorol.* **2019**, *268*, 146–155. [CrossRef]
54. Mainuddin, M.; Kirby, M.; Chowdhury, R.A.R.; Shah-Newaz, S.M. Spatial and temporal variations of, and the impact of climate change on, the dry season crop irrigation requirements in Bangladesh. *Irrig. Sci.* **2015**, *33*, 107–120. [CrossRef]
55. Bouregaa, T. Impact of climate change on yield and water requirement of rainfed crops in the Setif region. *Manag. Environ. Qual. Int. J.* **2019**, *30*, 851–863. [CrossRef]
56. Chen, X.; Wang, L.; Niu, Z.; Zhang, M.; Li, C.a.; Li, J. The effects of projected climate change and extreme climate on maize and rice in the Yangtze River Basin, China. *Agric. For. Meteorol.* **2020**, *282*, 107867. [CrossRef]
57. Ma, J.Q.; Li, P.F.; Liu, L. Experimental Study on Crop Coefficient of Summer Maize in Henan Province. *Water Sav. Irrig.* **2016**, *4*, 24–27. (In Chinese)